

Reducing Agents in Colloidal Nanoparticle Synthesis – an Introduction

GONZALO VILLAVERDE-CANTIZANO^a,
MARCO LAURENTI^a, JORGE RUBIO-RETAMA^a AND
RAFAEL CONTRERAS-CÁCERES^{*a}

^aDepartment of Chemistry in Pharmaceutical Sciences, Faculty of Pharmacy, Complutense University of Madrid, 28040 Madrid, Spain

*E-mail: rafcontr@ucm.es

1.1 Historical Point of View

The fields of nanomaterials and nanotechnology appear to be breakthrough discoveries of this modern age, thanks in part to the multiple applications that are continually appearing almost day by day in fields as diverse as pharmaceuticals, nanomedicine, catalysis, and green energy, among others.¹ However, nanomaterials by themselves have existed for many years; indeed most of the current methodologies applied in the industry are approximations from the gold(0) nanoparticle synthesis experiments carried out by Michael Faraday in the 1850s through reduction of dissolved gold(III) cationic ions using a reducing agent, which obtained gold colloids. These experiments are based on three steps which are already fully valid in current processes: (1) the reduction of the starting ion into insoluble atoms; (2) the formation of a core through aggregation/saturation processes; and, finally, (3) the surface

growing process by diffusion of the reduced atoms from the nuclei and reduction/deposition process of the atoms from the solution to the most exposed surface by electronic transport from the reducing agent in the solution.²

Over the last 40 years, many methods have been developed for forming nanoparticles and nanomaterials, from different sources and using innumerable reagents, solvents, and conditions. The available methods can be classified as chemical, physical, biological, or a combination of all three. They can also be divided into two pathways of synthesis: the top-down approach mostly used by physical methodologies, where a bulk component is used as a starting material which is converted into nanoparticles through mainly physical methods, and the bottom-up approach mostly used in chemical and biological methods, where soluble material is reduced to insoluble nanoparticle dispersion.³ The presence of reducing agents and capping agents upon the use of bottom-up methodology is often essential for controlling the final properties of the nanomaterial product.

Reductants have the role of driving electrons from the solution to the ions (usually metallic ones) to form atoms. In other words, they reduce the salts into the reduced form, which is usually insoluble. The aggregation of insoluble atoms forms clusters that will grow to reach a nanoscale size. The obtained nanoparticles are most stable in dispersion.

The methods most used since the 1990s for the controlled chemical synthesis of nanomaterials have been carried out using a variety of chemical reagents, among which some are toxic. The chemicals employed have been NaBH_4 , N_2H_4 , aldehydes as formaldehyde; CO, ascorbic acid, hydroquinone, citrate, among others as reducing agents; and PPI (polypropylene polybenzyl isocyanate), PEI (polyethylene imine), CTAB (cetrimonium bromide), linoleic acid, oleylamine, PAA (poly(acrylic acid)), PAMAM (poly(amidoamine)), OA (oleic acid), TOPO (trioctylphosphine oxide), TOP (trioctylphosphine), *etc.* as capping agents. In certain cases, a given reagent can act in a dual role as capping and reducing agent at the same time. These structures, as well as the functional groups of this type of double agent, influence the kinetics of the reduction process and, as a consequence, the final properties of the system. Thus it is essential to study how this influence can be modulated to experimentally control the final material.⁶² Examples of solvents typically used are toluene, ethanol, DMF (*N,N*-dimethylformamide), *etc.* A combined careful selection of reducing agent/capping agent, solvent, and conditions such as temperature or reaction time allows control over the shape and size, obtaining different sizes of nanomaterials such as spherical nanoparticles, as well as anisotropic structures such as plate rattles, urchins, rods, wires with applications in catalysis optics or nanomedicine, among others.^{4,5}

In the majority of these methods, reducing agents are used in excess with regard to the stoichiometric quantities. This complicates the process, making the translation of this kind of technology to the industrial process more difficult. It is important to mention that the current tendency is to find reaction conditions where the reducing agent is also in charge of directing the structure and being a stabilizer of the final product. Thus the design of new agents is a field that is yet to be explored.⁶²

Nowadays, green chemistry in nanoparticle synthesis is an emerging field seeking to find its way toward wider use in industrial applications. In this manner, the search for greener reducing agents with the capacity to reduce and stabilize the nanoparticle dispersions in a controlled way is particularly pursued among synthetic chemists and material scientists. Thus, green chemistry has influenced the design of nanoparticle synthesis routes in the last decade. The necessity of obtaining new and more eco-friendly pathways for affording nanoparticles in a scalable and controllable way gives nanoparticle biosynthesis a plausible chance for industrial application.

Indeed, over the past few decades, we have witnessed exceptional developments in the production of nanomaterials with well-controlled morphologies. In addition to chemical naturalness and crystalline quality, the morphology of these nano-sized solids is an important factor that regulates their physicochemical properties. For the preparation of metal nanoparticles, bottom-up liquid-phase techniques are very interesting because they are versatile and easy to use. They also allow accurate control of the structure, chemical nature, and morphology of the resulting particles, and among the various methods for synthesizing nanoparticles in solution the “polyol process” can be easily upscaled. This is of particular importance for the industrial synthesis of nanoparticles, which generally requires that the processes are carried out with only a few process steps and using the cheapest, least amount of raw material possible. Several preparation methods rely on the use of medium to strong reducing agents such as alcohols, citrate ions, hydrazine, or sodium borohydride to reduce the metal precursor. These methods are usually run in a low boiling solvent, making it difficult to obtain well-crystallized particles; thus, subsequent heat treatments are required. Furthermore, although these reduction reactions can be performed under specific conditions, such as those associated with microemulsion techniques, to achieve a very small dispersion size, the large volume of solvent used in the synthesis seriously hampers large-scale production.^{6–9}

1.2 Polyols

Polyols have emerged as a very useful class of compounds for the preparation of metal nanoparticles in what is known as the “polyol process”.¹⁰ The upside of this method is that the polyol can act as a solvent for the solid precursor and as a reducing agent. Certainly, the pioneers in this field are Fiévet, Lagier, and Figlarz, who demonstrated that polyols reduce the ions of noble metals and copper, and even more electropositive metals such as cobalt or nickel, to a zero-valent state. After 30 years of the polyol method, we now have a good overview of its capabilities for producing metal particles. The polyol medium offers many advantages, such as: (1) its high boiling point allows synthesis at a relatively high temperature, ensuring that well-crystallized materials are obtained; (2) the reducing medium protects the prepared metal particles from oxidation; (3) it has the ability to coordinate the metal precursors and the surface of the particles, minimizing coalescence; and (4) it has

a high viscosity that favors a controlled diffusion regime for particle growth, resulting in controlled structures and morphologies.¹¹

The study of the polyol process has permitted subject specialists to identify several steps and key points during the reaction: (1) the dissolution of the metal precursor which can occur at room temperature or during the heating phase; (2) the possible formation of an intermediate-acting cationic deposit; (3) the nucleation stage of monomeric species; and (4) the growth stage leading to the formation of metal particles. The presence of OH groups gives the polyols coordination properties which can compensate for their lower polarity compared to water. Furthermore, polyols can be adsorbed on the surface of particles, especially in oxides, providing excellent colloidal stabilization that makes it possible to control the nucleation, growth, and agglomeration state of particles. The high viscosities of polyols such as ethylene glycol (EG) ($\eta = 16.1$ mP s) concerning water ($\eta = 0.890$ mP s) are also advantageous for controlling such processes. The high boiling point of polyols allows synthesis to be carried out at a temperature of 197 °C for EG, up to 328 °C for tetraethylene glycol. Often the use of such a high reaction temperature leads directly to crystalline nanomaterials, without the need for post-annealing.¹²

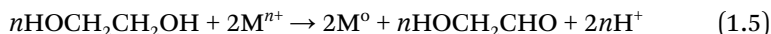
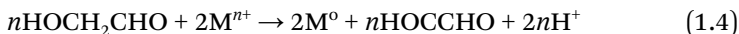
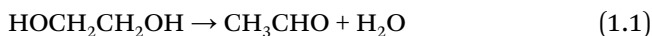
Generally, in the polyol method metal salts are used as raw materials, with different counter-anions such as chloride, nitrate, sulfate, hydroxide, and acetate. The identification of the compounds formed after the introduction of the precursors of the metals in solution is very relevant, because they influence the thermodynamics of the reaction as well as the reduction kinetics. The affinity of polyol molecules for different metals and different nuclei facets can also affect the shape of the seeds and/or the final size and morphology of the particles. The presence of the O-CH₂-CH₂-O group in most polyols strongly favors chelates because it provides the five-membered metallacycles which are the most thermodynamically stable.¹⁰

The coordination ability of polyols improves the solubility of metal ions through the formation of metal complexes. At the same time, the complexation of the polyol with the metal center is facilitated by deprotonation of the hydroxyl group by a base such as OH, or by the counter ion itself when acetate precursors are used. For metal salts that may not be very soluble (such as hydroxides or acetylacetonates), increasing the reaction temperature can improve the solubility enough to allow the reaction to proceed.

Upon heating a reaction mixture, two cases must be distinguished: for 3d transition metals (Fe, Co, Ni, Cu) a solid intermediate of the phase precipitates, while for noble metals no such precipitate is observed.^{13,14} Experimental evidence attributes a kinetic role to these intermediate phases in the reaction mechanism. These solids act as deposits of metal cations and their dissolution controls the concentration of the dissolved metal species which are reduced. The nucleation phase corresponds to the formation of the first groups or nuclei. The syntheses are generally carried out with species possessing oxidation numbers above zero, making a reduction step necessary. However, it is still sometimes unclear whether there is a prior reduction of solvated metal species to produce metal atoms in solution which further lead to the nuclei, or whether the unreduced metal species combine first to

generate seeds which are reduced in a second step.¹⁵ The growth of mono-disperse particles is generally explained by the LaMer and Dinegar nucleation and growth model, where nucleation and growth are assumed to be two separate processes.¹⁶ This hypothesis is still valid for polyol-mediated syntheses because narrow size dispersions are generally observed. Most of the time the particles are not aggregated, thanks to the use of capping agents that encapsulate the nanoparticles and because the presence of the polyol molecules on their surface makes coalescing difficult. For noble metals, growth generally occurs at a lower temperature than for other metals due to their specific reduction potential. In general, the particles obtained using the polyol method show a high crystallinity without the use of autoclaves and post-annealing.¹⁰

A crucial aspect of the polyol synthesis is the redox process by which the precursor of the metal is reduced. In a typical redox process, the chemical reduction of a salt precursor by a reducing agent needs an electron transfer between two chemical species (*i.e.* electron donors and acceptors), which is driven by the difference in their reduction potentials (ΔE).⁶² For a reduction in which a polyol is involved, the mechanism largely depends on the reaction temperature, in which different derivatives can be involved at different temperatures, as shown in eqn (1.1)–(1.5). Depending on the reaction temperature of EG, which acts as a reducing agent, the reactive species and intermediates are different. If the reaction is carried out at a temperature >160 °C, the EG is dehydrated to generate acetaldehyde, as shown in eqn (1.1),⁶ after which the acetaldehyde obtained is responsible for the reduction of metal ions, accompanied by its oxidation to diacetyl.^{7,17} The species are different if the reaction temperature is between 140 °C and 160 °C, where glycolaldehyde becomes the main reducing agent that can be generated by heating EG in air,⁸ and thus serves as a reductant to reduce metal ions while oxidizing to glyoxal.⁹ When the reaction temperature is below 140 °C, EG can act alone as a reductant, leading to the formation of glycolaldehyde as an oxidized product.¹⁰



Figlarz's group was the first to publish a work on the synthesis of noble metal nanoparticles using polyol in the early 1990s (Table 1.1). Spherical nanoparticles of Au, Ag, Pd, and Pt were prepared with different dimensions

Table 1.1 Room temperature oxidation and reduction potentials (V versus SCE) measured using a rotating disk electrode and aqueous standard potentials for the reduction of metallic compounds. Adapted from ref. 22 with permission from Elsevier, Copyright 1999.

	E (V vs. SCE) ^a in ethylene glycol-KNO ₃		Aqueous std. pot. (E vs. SCE)
	Pt electrode	Carbon electrode	
EG ox.	2.00	1.65	
AuCl ₄ ⁻ /Au red.	0.65	0.62	0.74
Ag ⁺ /Ag red.	0.34	0.33	0.55
PtCl ₆ ²⁻	-0.22	-0.22	0.46 ^b
Pd(NH ₃) ₄ ²⁺ /Pd	-0.68	-0.80	0.24
EG red.	-0.82	-1.15	

^aSCE: saturated calomel electrode. ^bCalculated from the potentials of the following two couples: PtCl₆²⁻/PtCl₆⁴⁻ and PtCl₆⁴⁻/Pt.

in EG, with PVP (polyvinylpyrrolidone) as a capping agent.^{18–21} As already mentioned, the polyol synthesis is based on a redox process; however, it was not until the work of Bonet *et al.* that the reduction potential of several noble metal salts in EG was investigated. They studied the electrochemical behavior of EG and determined the reduction potential of AuCl₄⁻, Ag⁺, PtCl₆²⁻, and Pd(NH₃)₄²⁺ at 20 °C by linear scanning voltammetry (Table 1.1).²² Additional electrochemical potentials of various reductants can be found in Table 1 of ref. 62.

Those authors found that reduction potential becomes more negative in the following order: AuCl₄⁻ > Ag⁺ > PtCl₆²⁻ > Pd(NH₃)₄²⁺, and that EG oxidation started at more positive potentials than metal reduction, suggesting that it cannot reduce these noble metals. However, even at room temperature, it was possible to observe and obtain Ag and Au nanoparticles using EG as reducing agent. This discrepancy was attributed to the fact that the measurement of the potential is the sum of the thermodynamic potential and the overpotential, which is not negligible. Regarding the synthesis of anisotropic nanoparticles, Xia's group made a significant contribution. Except for Ru, all noble metals have a face-centered cubic phase (fcc) in which there is no inherent driving force for the growth of anisotropic forms. In fact, according to Wulff's construction, the thermodynamically favored form of a metallic fcc under vacuum is a cuboctahedron. Much effort has been made to understand the mechanisms by which nanoparticles form under kinetic control. In general, the use of polyol alone is not sufficient to control particle size and shape. For this reason, several strategies were developed to control size and morphology using protective agents, kinetic control on reduction, and oxidative etching.¹⁰

For the production of Au nanoparticles, the polyol method often requires the use of PVP, which has a crucial impact on the size and aggregation, but also on the shape of the resulting particles. In fact, a high PVP:Au precursor ratio results in the coverage of all Au facets and therefore in isotropic growth and formation of spherical nanoparticles.¹⁸ To obtain anisotropic growth, a lower PVP:Au ratio should be used. Employing these conditions, the selective interaction between PVP and the different crystallographic

planes of Au nanocrystals can reduce the growth rate in the $\{111\}$ direction and increase it in the $\{110\}$ direction, leading to large triangular or hexagonal Au nanoplates.^{23,24}

Although 1D nanostructures for Au in polyols have never been documented, other morphologies have been obtained by varying the capping agent, through replacing EG with heterogeneous glycols, or by using heterogeneous nucleation processes. In order to acquire small Au nanoparticles, a low concentration of AgNO_3 can be added to a 1,5-pentanediol solution containing HAuCl_4 and PVP. Octahedra, truncated octahedron, cuboctahedra, or cubes can be obtained by varying the Ag:Au ratio, with an average nanoparticle size in the range of 60–140 nm. Furthermore, it has been shown that Au decahedra, icosahedra, and truncated tetrahedra can be obtained by substituting the polyol (DEG (diethylene glycol) and TTEG (tetraethylene glycol)) and varying the ratio of HAuCl_4 :PVP.^{25–27}

Non-aggregated and monodisperse Ag nanoparticles were obtained easily using EG as reductant and solvent, silver nitrate as the metal precursor, and PVP as a capping agent. Unlike gold, 1D Ag nanostructures with well-controlled size and aspect ratios have been synthesized in polyols.²⁸ Hexachloroplatinic acid was used as a nucleating agent with a Pt:Ag ratio of 10:3. The anisotropic growth is due to the selective adsorption of PVP to a particular plane or edge of the Pt seeds before the metallic silver is deposited in the planes not covered by the PVP, which acts as a protective agent. The thickness of the nanotubes varies with the AgNO_3 :PVP ratio.

Over the past decade, the polyol process has been modified by Xia's group to gain better control over the nucleation and growth phases of silver nanoparticles.^{29–31} By varying several parameters such as the Ag:PVP ratio, reaction temperature, seeding, and growth conditions, it has been possible to synthesize nanocubes, nanowires (NWs), nanobars, cuboctahedra, and bipyramids.^{29–32} The reproduction of these structures is illustrated in Figure 1.1.

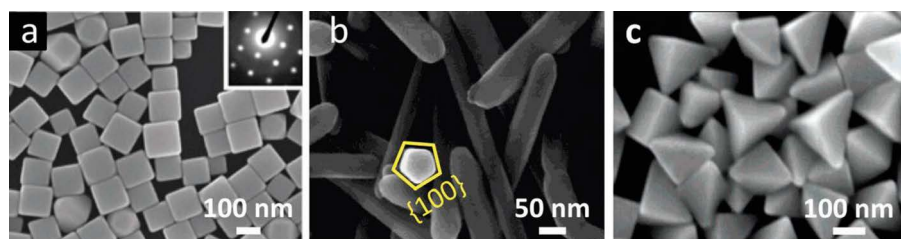


Figure 1.1 (a) SEM image of Ag nanocubes. SAED (selected area electron diffraction) pattern obtained from TEM studies is given in the inset. Reproduced from ref. 30 with permission from American Chemical Society, Copyright 2004; (b) SEM image of silver NWs with a pentagonal cross-section. Adapted from ref. 32 with permission from American Chemical Society, Copyright 2003; (c) SEM images of Ag bipyramids. Adapted from ref. 33 with permission from American Chemical Society, Copyright 2006.

The reaction and growth mechanisms involved in this synthesis were analyzed in a review by Xia *et al.* To produce Ag nanocubes, the AgNO_3 concentration must be relatively high and the PVP: AgNO_3 molar ratio should be low. These conditions result in rapid nucleation and growth of silver seeds.³⁴ The selective adsorption of PVP on the $\{100\}$ facets will lead to the preferential addition of silver atoms to the $\{111\}$ facets with the formation of cubic particles (Figure 1.1a). Nanorods and NWs can be synthesized by homogeneous and heterogeneous nucleation, adopting different strategies such as the use of Pt and/or Ag seeds in PVP/EG solutions.³⁵ Larger silver nanoparticles can then grow into pentagonal nanorods and eventually form NWs due to the Ostwald ripening process (see Figure 1.1b). Finally, the key to producing Ag nanobipyramids with an average edge length of 75–150 nm was the addition of NaBr to EG containing AgNO_3 and PVP (Figure 1.1c). The edge length was varied by changing the reaction time.³³

Transparent Ag NW electrode films are believed to represent a promising alternative to transparent indium tin oxide electrodes. To achieve the required electrical and optical characteristics, Ag NW with a small diameter and large format is desirable. Significant results were obtained with the heterogeneous nucleation of silver chloride, mediated by adding NaCl to the polyol before silver nitrate.³⁶ The polyol process to synthesize anisotropic Ag structures using templates is a very useful method. In fact, using this process it is possible to obtain assembled Ag NWs by reducing silver thiolate in a biphasic 1,2-propanediol/toluene containing dodecanethiol.³⁷ The NWs are formed at the polyol/toluene interface after aging. Another paper reporting a one-step synthesis of silver NWs was published by the Fiévet group. They used hexagonal mesoporous silica SBA-15 as a template and obtained NWs as single crystals with $\{111\}$ metallic silver planes along the wire, and a diameter equal to the pore diameter of the mesoporous silica.³⁸

Bonet *et al.* obtained Pd nanoparticles with a 10 nm diameter using PVP as a protective and stabilizing agent to avoid nanoparticle aggregation in the presence of EG at 100 °C.²¹ Spherical nanoparticles with a diameter size of 5.5 nm self-organize into 50 nm Pd nanoflowers when synthesized from $\text{Pd}(\text{acac})_2$ in a mixture of oleylamine/*o*-dichlorobenzene/1,2-hexadecanediol at 180 °C.³⁹ Xia's group was one of the main groups involved in the development of the synthesis of anisotropic nanoparticles of Pd.^{40,41} The key of the process lies in the oxidative power of O_2 which has been modulated by changing the pH with HCl, or by adding ionic species such as FeCl_3 . The O_2/Cl couple acts as an oxidative etching agent on the Pd nanoparticles in the first phase of the reaction and helps to remove twinned particles. Uniform monocrystalline cuboctahedra were obtained after a three-hour reaction.⁴⁰ However, the $\text{O}_2\text{-Cl}$ etching alone does not slow the reduction sufficiently to allow anisotropic growth. Tight control of the rate of reduction was achieved by introducing iron(III) as an additional oxidative attack agent; this favors the formation of anisotropic structures rather than thermodynamically favored ones. The Fe(III) concentration plays an important role in controlling the reduction kinetics and therefore the morphology of the Pd nanostructures.⁴¹

Besides, the increase of Fe(III) amount considerably reduces the number of seeds through the oxidative attack and allows the formation of larger nanocrystals.⁴²

Platinum is probably one of the most studied noble metals due to its remarkable properties and applications. Pt has found widespread use as a catalyst in many industrial processes, such as the reduction of polluting gases emitted by cars, the synthesis of nitric acid, oil cracking, biosensors, and recently in proton-exchange-membrane fuel cells, of great importance to the automobile industry. For this reason, much effort has been made to synthesize supported and well-dispersed Pt nanoparticles with a small size distribution.⁴³ In 2003, Laine and Sellinger were the first to patent the synthesis of Pt and Ru nanoparticles based on the polyol process. By introducing additives such as PVP, they avoided particle aggregation and reduced the size of the nanoparticles to achieve high dispersion. Hexachloroplatinic acid, often used for the synthesis of Pt nanoparticles, is stable in EG at room temperature, but can be easily reduced when the temperature rises above 100 °C. As already mentioned, PVP is used as a steric stabilizer and shape-controlling agent. The electrostatic stabilization can be achieved through the use of sodium acetate.^{21,44} In EG/PVP, the size of the Pt nanoparticles can be controlled by varying the concentration of the Pt precursor or PVP. For example, the size of the nanoparticles increases with the concentration of Pt precursor, while for a fixed concentration of Pt precursor, as the concentration of PVP increases, the particle size decreases and then increases rapidly. When the reduction of metal salts is relatively rapid, the nanocrystalline seeds tend to grow and generate the thermodynamically favored form in order to minimize the surface energy.⁴⁵ Song *et al.* demonstrated that the addition of AgNO₃ improves growth along {100} and/or suppresses growth in the {111} directions, and by varying the concentration of AgNO₃ they prepared cubes with a reduced size distribution.⁴⁶ Wang *et al.* have proposed an alternative to the use of a protective polymer of this type, which in some cases can be harmful to other applications. They synthesized unprotected Pt nanoclusters with sizes between 1 and 2 nm and narrow size distribution. The synthesis was carried out in EG in the presence of NaOH (pH < 12) and the product could be easily separated from the solvent and further dispersed in an organic solvent to form stable suspensions.⁴⁷ The synthesis of nanoparticles of Pt with an anisotropic structure in EG has been extensively studied using PVP almost systematically to prevent aggregation and flocculation. The control of Pt nanoparticle morphology is highly dependent on the speed of the atom supply: like Pd, it can be manipulated by oxidative etching using oxidative ions such as O₂/Cl. The diffusion rate of the atom also depends on the temperature, and therefore different morphologies are obtained simply by varying the reaction temperature. Similarly to Ag and Pd, Xia's group demonstrated that controlling the rate of reduction allows one to produce anisotropic Pt morphologies. In fact, the syntheses of star-shaped branched multipods and NWs were obtained only by coupling the polyol reduction of a platinum precursor, in the presence of PVP, with a redox pair of Fe(II)/Fe(III),

while oxygen was also needed to regenerate the redox pair.^{48,49} It is important to note that, unlike Ag and Pd, the reduction of a Pt(IV) precursor proceeds through a two-step process and involves intermediate Pt(II) species. In this two-step process, the key parameter is the stabilization and control of intermediate species to slow down the reaction. In general, as the reduction becomes slower, the growth of the {111} planes increases, leading to the formation of highly anisotropic nanostructures.

Rh nanoparticles have very high surface energy and the control of size and shape is difficult and requires special conditions.⁵⁰ The oxidative mechanism has already been detailed for the synthesis of nanoparticles from Ag, Pd, and Pt, which are also valid and quite similar for Rh nanoparticles. Somorjai *et al.* were the first to synthesize Rh nanoparticles with well-controlled size and shape using the polyol process.⁵¹ Catalytically active (less than 10 nm) Rh nanocrystals with high selectivity (>85%) were obtained using trimethyl(tetradecyl)ammonium bromide (TTAB) as the surfactant in EG. In the presence of TTAB, Br ions stabilize the Rh {100} surface, inducing the formation of nanocubes.⁵¹ Schaak *et al.* obtained different sizes and shapes of Rh nanoparticles by varying the polyol and Rh precursor under an inert atmosphere of Ar to avoid oxidative etching. By modifying the polyol and the Rh precursor, they were able to obtain cubes (RhBr₃ and DEG), icosahedral (Rh₂(COOCF₃)₄ and EG), and triangular plates (RhCl₃ and TEG).⁵² In a different work, Biacchi *et al.* isolated Rh clusters with diameters from 1 to 2 nm and used them as seeds to differentiate between the nucleation and growth phases and obtain different morphologies of Rh nanoparticles. In this work, they propose that anionic ligands influence the crystallographic planes and the degree of crystallinity of the final particles.⁵³ Concave Rh nanocrystals formed by the dissolution of convex cubes have been proposed by using two different approaches: overgrowth and dissolution.⁵⁴ These two strategies are very similar except for the type of crystal face involved, which can lead to a great variety of shapes. Xia's group obtained an original morphology using a model-directed path to generate Rh nanoframes with a highly open structure (Figure 1.2a).⁵⁵

Cubes of Pd were used as seeds for nucleation and growth of Rh, which only settles in corners and edges due to the presence of Br ions. The Pd template was removed using an etching agent based on a Fe(III)/Br couple in aqueous solution, with the addition of HCl to avoid the formation of insoluble Fe(OH)₂. The precise shape control of Rh nanoparticles offers an efficient path to optimize its catalytic performance.

Ru can crystallize as a hcp or fcc structure. For this reason, the anisotropy of the hexagonal system is expected to generate anisotropic crystals. However, there are only a few works on anisotropic Ru nanoparticles. Usually, by using RuCl₃ as the precursor, and without a protective agent, the synthesized particles are in the submicrometric range. However, the addition of a surfactant allows one to obtain isotropic Ru nanoparticles with a diameter between 1 and 6 nm.⁵⁶ Colloidal nanoparticle suspensions of stable ruthenium can be obtained by using PVP or acetate or by adding NaOH during synthesis, resulting in stabilization from electrostatic repulsion.^{47,56,57} As the concentration of the precursor or the reaction temperature increases, the size of the

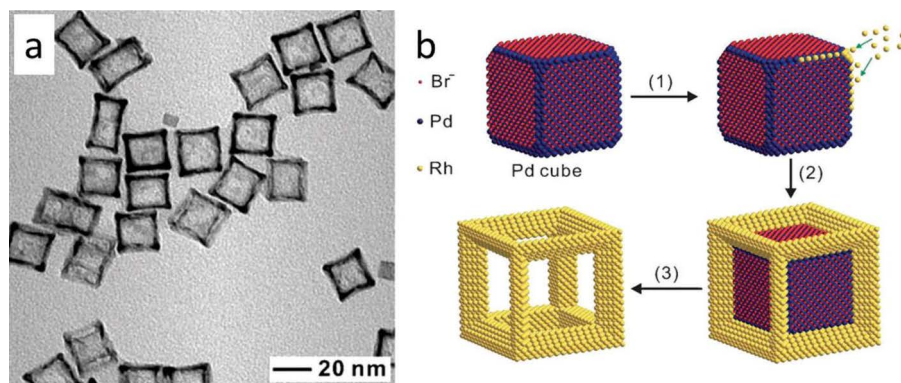


Figure 1.2 (a) TEM picture of the Rh nanoframes obtained by selective etching of the Pd cores from the Pd-Rh core-frame NCs; (b) corresponding steps of formation: (1) selective nucleation of Rh; (2) formation of bimetallic Pd-Rh core-frame concave NCs; (3) formation of cubic Rh nanoframes by selectively etching away the Pd cores. Adapted from ref. 55 with permission from John Wiley & Sons, Copyright 2012 WILEY-VCH Verlag GmbH & Co. KGaA, Weinheim.

nanoparticles generally decreases. This effect can also be induced by changing the polyol and consequently the reflux temperature. Yan *et al.* showed that the particle size decreases from 5.4 nm to 2.9 nm and then to 1.8 nm, when the boiling point of the polyol increases from 198 °C to 245 °C and then to 285 °C using EG, DEG, and TEG.⁵⁸

Iridium is the known material with the highest corrosion resistance. However, it is a very rare material and it is mainly used in alloys for specific applications due to their conductive nature. These alloys are therefore potential electrocatalysts which can be used as catalysts for oxygen-evoking anodes in the proton-exchange membrane. They have been synthesized into polyols with both conventional and heated microwaves.^{59,60}

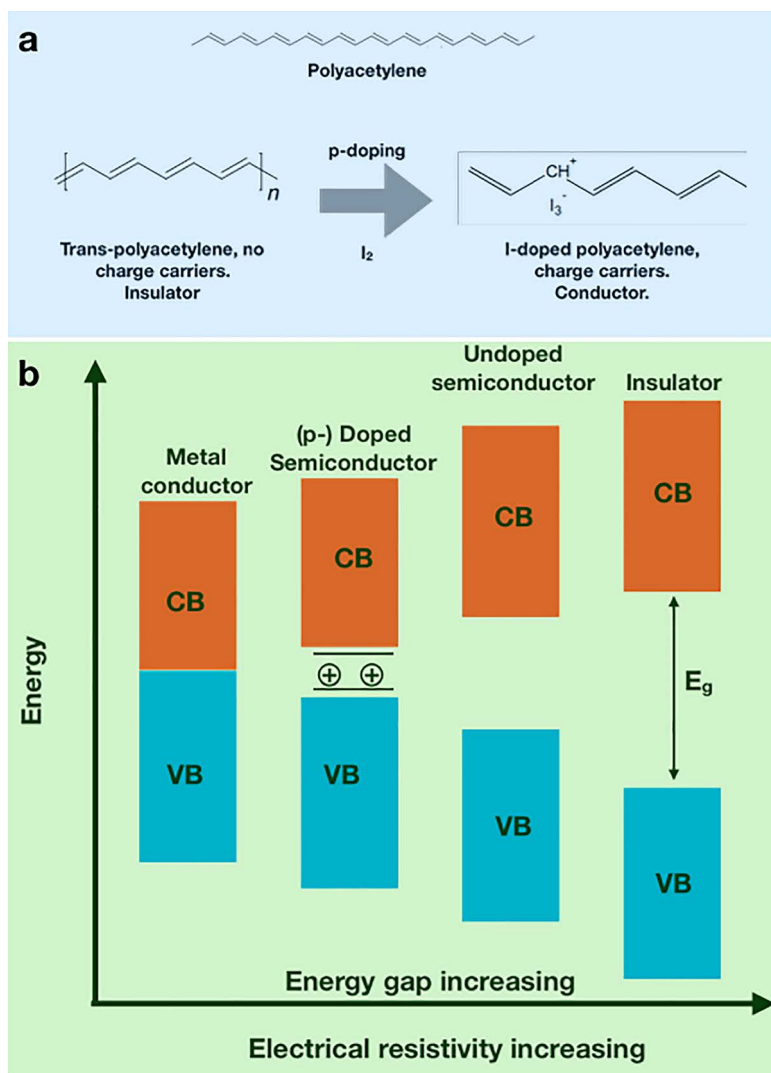
1.3 Redox Potential on Polymer Nanoparticles

Polymers are molecules of high molecular weight constituted by the repetition of small subunits called monomers. Most of these molecules acquire globular conformation when they are dispersed in good solvents, rendering the so-called polymer nanoparticles, which can be applied in different applications ranging from nanomedicine to electronics.⁶¹

Investigations have been focused on the action mechanism that triggers the increase of the conductivity in polymers. This phenomenon was named doping and occurred when a halogenation process was carried out over the crystalline fibers of polyacetylene.^{63–65} This is a clear example of “p-doping”, where an oxidizing agent transforms a neutral polymer chain into a polymeric cation, which is neutralized by the reduced form of the oxidizing agent.⁶⁶ That process provides charges that are free to move under an applied electric field, rendering conductivity. The doping effect is accompanied by a

reduction of the energy gap between the top of the valence band and the bottom of the conduction bands that also affect the redox potentials of the material. Scheme 1.1 summarizes the effect of the energy gap increasing and its subsequent increment of the electrical resistivity.

After that, chemists realized that the use of a heteroaromatic ring permits the design of undoped polymers with inherent semiconducting properties. That opens a second route toward fine-tuning the electronic properties of

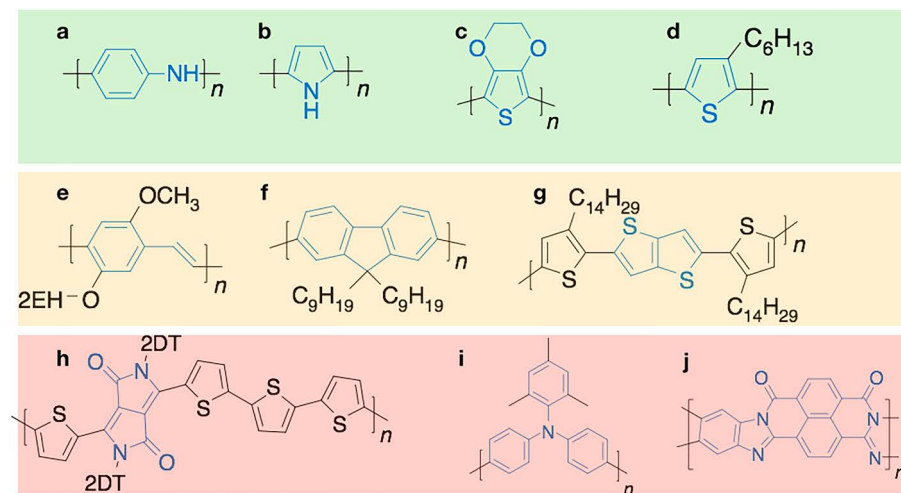


Scheme 1.1 Schematic representation of: (a) doping process for polyacetylene with iodine and its subsequent transformation into a conducting polymer by the presence of charge carriers; (b) bandgap structure of different materials as a function of the doping degree. The graph represents the increment of the energy gap that occurs when doping is reduced, making the system evolve from a conductor to an isolator.

this material.⁶⁷ Scheme 1.2 shows the most common conducting polymers based on the heteroaromatic structures.

The big advance of this new class of conducting polymer was the possibility of tuning the redox potential and bandgap of the polymers, opening a myriad of applications like antistatic coating, organic light-emitting panels, flexible photovoltaic panels, organic thin-film transistors, and electrode materials, among other implantable bioelectronics, which move a global market greater than \$200 million. For example, Table 1.2 shows the oxidation and reduction potential of the most representative conducting polymers.

Although the nature of the structure can define the redox potential of the polymers, further modifications in the monomers can vary the redox potentials of a specific family of conducting polymer, varying its possible applications. In this specific case, the PPV (polyphenylvinylene) is a clear example of such modifications.⁷² PPV represents a family of conducting polymers that can be considered as an intermediate between polyphenylene (PP) and polyacetylene (PA). However, in stark contrast to PP and PA, the modification of the chemical structure of both monomers by the introduction of lateral groups has permitted an increase in the processability of the fibers and has altered the electrochemical oxidation and reduction potentials of these polymers, which is related to the presence of electron donor or electron-withdrawing groups. Table 1.3 depicts the structure of some PPV derivates and the oxidation and reduction potential exhibited by each one.

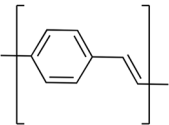
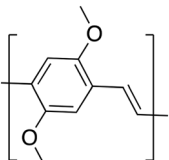
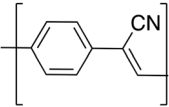
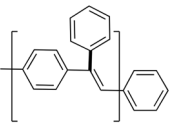
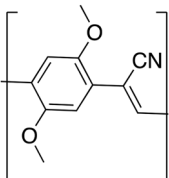


Scheme 1.2 Chemical structure of conducting polymer based on heteroaromatic rings: (a) polyaniline (PANI); (b) polypyrrole (PPy); (c) poly(3,4-ethylenedioxythiophene) (PEDOT); (d) poly(3-hexylthiophene) (P3HT); (e) poly[2-methoxy-5-(2-ethylhexyloxy)-1,4-phenylenevinylene] (MEH-PPV); (f) poly(9,9-dinonyl-9H-fluorene-2,7-diyl) (PF); (g) poly(2,5-bis(3-tetradecylthiophen-2-yl)thieno[3,2-*b*]thiophene) (PBTtT); (h) poly{[2,5-bis(2-decyltetradecyl)pyrrolo[3,4-*c*]pyrrole-1,4(2*H*,5*H*)-dione]-*alt*-[2,2':5',2'':5'':2'''-quaterthiophene]} (DPP-TT2); (i) poly(triaryl amine) (PTAA); (j) poly(benzimidazobenzophenanthroline) (BBL).

Table 1.2 Oxidation and redox potential of representative conducting polymers.

Polymer	$E_{\text{ox}}(\text{V})$	$E_{\text{red}}(\text{V})$	Reference
Poly(acetylene)	0.4	-1.1	68
Polypyrrole	0.35	-0.36	69
Poly(aniline)	0.4	-0.1	70
Poly(3-hexylthiophene)	n/a	0.70	71
Poly(phenylvinylene)	0.8	-1.8	72

Table 1.3 Examples of some polymer structures with their corresponding redox potentials.

Polymer	$E_{\text{ox}}(\text{V})$	$E_{\text{red}}(\text{V})$
	0.8	-1.8
Poly(<i>p</i> -phenylenevinylene)		
	0.70	-1.64
Poly(2,5-methoxy)-1,4-phenylenevinylene)		
	1.6	-0.96
Cyano-poly(<i>p</i> -phenylenevinylene) (CN-PPV)		
	1.17	-1.8
Phenyl-poly(<i>p</i> -phenylenevinylene) (Ph-PPV)		
	1.38	-0.86
Cyano-poly(2,5-methoxy)-1,4-phenylenevinylene		

In summary, nowadays conducting polymers constitute an important field of research due to the scientific and industrial interest. Further, their use in nanoparticle synthesis is now widely spread. For example, Ag nanoparticles have been synthesized through silver ions reduction by polyaniline (PANI) colloids in an efficient way, thanks to the reactive aryl-amine groups.⁷³ Other amine-based electron conductor polymer colloids have also recently been used with the same aim, such as the poly (propylene imine) (PPI) dendrimers that have been applied for the synthesis of Au nanoparticles. In this case, the PPI dendrimer-bearing amine groups interact with the gold salt, acting as a reducing agent but also as a stabilizer through their deposition into the resulted gold nanosphere surface.⁷⁴ Elsewhere, the field of biopolymers is opening a new horizon for nanoparticle synthesis: carboxymethyl cellulose (CMC) is also used both as a capping and a reducing agent for the gold nanoparticle synthesis, forming hybrid biodegradable nanomaterials with multiple applications in biomedicine.⁷⁵

These sorts of polymeric nanoparticles are characterized by their conducting properties and redox potentials, which dictate their applications and allow their use not only in nanoparticle synthesis but also in microelectronics, solar panels, electrode batteries, *etc.* in an industry worth more than \$200 million per year – which gives an idea of the importance of this kind of material.

1.4 Biological Materials (Plant and Leaf Extracts) – Nanoparticle Phytosynthesis

Phytosynthesis by plant extracts constitutes a very interesting strategy in green nanoparticle synthesis. Extracts from leaves, fruit seeds, even flowers are involved in the various nanoparticle synthesis mechanisms included in these methodologies.⁷⁶

The bio extracts have shown a powerful potential in metal accumulation and antioxidant properties. Their behavior mainly depends on their composition, which is a mixture of biomolecules such as polyphenols, flavonoids, quinines, tannins, enzymes, surfactants, lipids, small molecules like alkaloids or terpenoids, *etc.* which can play different roles such as reductants, oxidizers, and stabilizers among others. This methodology represents a useful alternative to the classic nanoparticle synthesis. It is based on the interaction of the leaf extract biomolecules with the starting material by redox reaction and afterwards a stable bond formation between the nanoparticle and the biomolecules acting as stabilizers (see Figure 1.3).

Further, the possibility to control the size, shape, and functionalization of the resultant material is sometimes easier than in other synthetic options, mostly due to the wide quantity of plants that have these properties. Depending on the leaf extract, the resulting nanoparticles will have different sizes, shapes, and secondary properties.

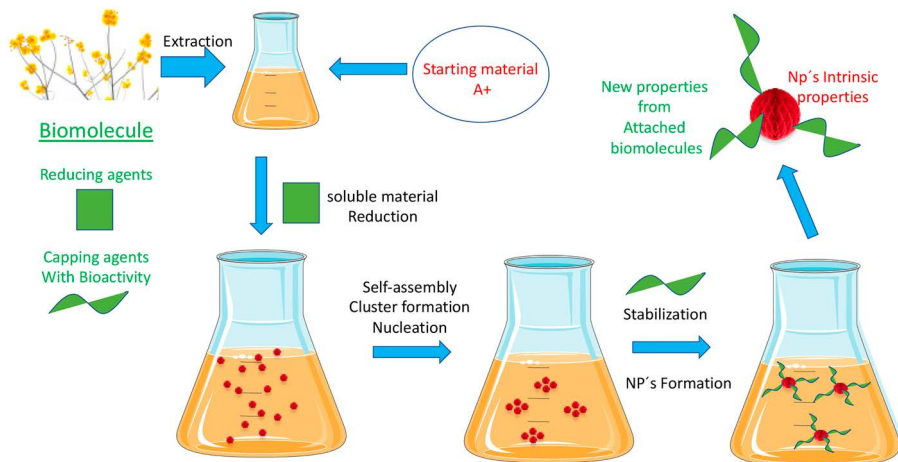


Figure 1.3 The process of using plant extract compounds as reducing/structure as well as director and stabilizer agents. The final nanomaterial possesses the acquired properties of the active capping agents.

Phytosynthesis is a nanoparticle synthesis pathway with promising traits for industrial adaptation, thanks to its low cost and eco-friendly nature, taking into account that the reducing and capping agents for the nanoparticle synthesis usually come from biomass wastes and the isolation of the final product is usually easier than in other methodologies, without complex workup processes. On the other hand, depending on the solvent, the temperature, and the rest of the extraction conditions used for the extraction process (pH, concentration, pressure), the reagent mixture will consist of different compounds.

Finally, the properties of the final nanomaterial may be improved by the physisorbed or attached substances coming from the plant extract. These molecules present in the nanoparticle's surface confer new properties, paving the way for a new application. For example, Tekin *et al.* described a green synthesis of silver nanoparticles with eugenol previously extracted from a clove bud. Eugenol is a phenylpropanoid compound found in a variety of plants, usually in its oxidized form, presenting a hydroxyl at the aromatic ring.⁷⁷ It has several properties for its application in medicine, being anti-inflammatory, antibacterial, antifungal, and antioxidant, thanks to its ability to absorb free radicals. In this case, eugenol was used as a reducing agent and the final material demonstrated an improved antibacterial effect *versus* Ag nanoparticles synthesized from classical pathways.⁷⁸

Cu nanoparticles are sometimes synthesized through treatments with leaf extracts; there are wide-ranging reports in literature with thousands of possibilities. The properties of the final copper nanoparticles normally vary based on the biomolecules that are finally fixed in their structure, but also, logically, on the different geometry that they have depending on the synthesis treatment. Table 1.4 shows some examples of nanoparticle phytosynthesis.

Table 1.4 Some examples of nanoparticle synthesis by reduction with plant extract.

Nanoparticles	Plant	Reducing agent	Reference
Iron, iron oxide	<i>Punica granatum</i>	Alkaloids flavones, proteins (reducing and capping agents)	79
	<i>Tea</i>		80
Gold	<i>Eucalyptus</i>	Proteins	81
	<i>Fruits</i>		81
	<i>The root from Morinda citriflora</i>		81
	<i>Sargassum</i>	Functional groups from components such as amine, alcohol, or carbonyls	1
	<i>Achillea wilhelmsii</i>	Alkaloids, flavones, proteins (reducing and capping agents)	82
Bimetallic gold–palladium	<i>Cacumen Platycladi</i>	Unknown	83
Silver	<i>Clove</i>	Eugenol	78
	<i>L.acapulcensis</i>	Alkaloids, flavones, proteins (reducing and capping agents)	84
	<i>Clitoria ternatea and Solanum nigrum</i>	Alkaloids, flavones, proteins (reducing and capping agents)	85
ZnO	<i>Cassia fistula and Melia azadarach</i>	Alkaloids, flavones, proteins (reducing and capping agents)	86
Copper chloride, copper sulfate, copper, copper acetate	<i>Extracts from several flowers, fruits, leaves, etc.</i>	Alkaloids, flavones, proteins (reducing and capping agents)	87

1.5 Miscellaneous Reductants

Microorganisms are one of the most promising tools for nanoparticle synthesis; bacteria, algae, fungi, and yeast are the typical living organisms used during the last decade. All of them have a reductase enzyme or several other molecules that provide and transport electrons for carrying out the redox bioprocess to generate nanoparticles.^{3,88,89}

The use of living cells as a reagent for nanoparticle synthesis has grown in recent years, mostly due to the possibility of their being genetically modified to afford the desired final nanoparticles. In general, bacteria, fungi, and algae have two ways of reducing ions in salt for nanoparticle synthesis: (1) intracellular reductase enzyme; (2) extracellular carbonyl groups from the cell wall (see Figure 1.4). Alternatively, the lipopeptide surfactin, present in the extracellular and intracellular matrices, acts as surfactant and stabilizer.

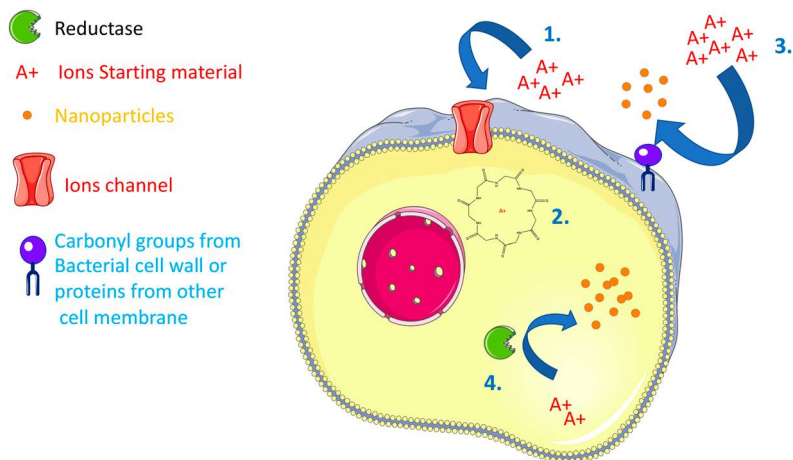


Figure 1.4 Different mechanisms of cells for forming metallic nanoparticles. 1. Active internalization of ions in the cells through ionic channels; 2. Accumulation of ions into the cytosol by stabilizing agents; 3. Fixing and reduction of ionic species by proteins of carboxylic groups present in the cell wall/cell membrane; 4. Reduction of the ions into the reduced insoluble species to form clusters in the nucleation process and finally afford a nanoparticle.

1.5.1 Bacteria

Usually bacteria can produce silver nanoparticles in both extra and intracellular pathways. Further, CdS nanoparticles have also been produced by bacteria through Cd^{2+} accumulation in the cytoplasm by the zinc channel and forming complexes with metalloproteins; later the cadmium is reduced by sulfite reductase.

Other metallic and oxide nanoparticles such as chromium and zinc oxide can also be produced by fungi, which have amazing catalytic properties. Gold nanoparticles were also synthesized in both extracellular and intracellular media by bacteria; however, the mechanism is not well defined, and this fact precludes the control of the nanoparticle features.⁹⁰

1.5.2 Fungi

Fungi offer distinct strategies to afford different kinds of nanoparticles. This biomaterial can generate metallic nanoparticles by extra and intracellular conditions, in *in vitro* and *ex vivo* media.

The use of dead fungal mass provides advantages that make this material very useful in the industry, because it doesn't need nutrients to keep the fungi alive during the process.⁹¹ Besides, the dead biomass is easy to handle and has a high capacity for wall-binding to the corresponding metal, so is easy to scale up thanks to the high amounts of enzyme secretion and the ability to accumulate large quantities of metals.

Yeasts are unicellular fungi widely used in the industry for multiple aims thanks to their easy handling in laboratory conditions. Yeasts use oxygen from different sources for growing, and this attribute can be exploited for the synthesis of metallic nanoparticles through the reduction process. Dead yeast material can also operate as a reducing agent thanks to its potential to absorb metallic ions and, once internalized, to be reduced. Still, this process is not evident in all parts of its mechanism.⁹²

In the case of these biomaterials, the most accepted mechanism suggested to occur is the enzymatic synthesis through NADPH-dependent nitrate reductase found in the case of the intracellular process. On the other hand, if the process is carried out in the extracellular matrix, the proteins from the cell surface will be able to fix and reduce the metallic ions. Nickel, copper, cadmium, and silver nanoparticles, among others, have been synthesized with these fungi materials as part of the bioremediation process, removing these heavy metals from the environment and using these ions for forming highly valuable new products such as metallic nanoparticles, which can be used in different fields such as biomedical catalysis, energy, *etc.*^{93–95}

1.5.3 Algae

Biosynthesis of nanoparticles by algae is a less explored field that has attracted more attention in recent years due to this material's potential as an accumulator of metallic ions. This property might be interesting for renewing permanent metallic waste into high-value products. In the literature, it can be seen that gold ions have been the most used as starting materials because algae present a high accumulation capacity for these ionic and metallic species. These microorganisms are able to reduce the toxic effects of the metallic bioaccumulation by concentrating the metallic salts into different organelles, reducing the cellular stress. On the other hand, algae present cyano sulfur and phosphorus in their cytosol, making it possible to reduce the gold ions to their atomic forms.

Furthermore, algae single proteins present in the cell wall also make possible the reduction of other ionic species such as cadmium, silver, or copper.⁹⁶

1.5.4 Proteins

Proteins, amino acids, and peptides are one of the most interesting groups of bioreagents for nanoparticle green synthesis. The proteins add their capacity to act as colloidal stabilizers to their redox potential. This fact makes the redox process easier: further proteins can finally be fixed to the surface of the nanoparticles, transferring some of their potential functions to the final material.⁹⁷

The determination of redox potential in the proteins is usually governed by the pK_a values and structure conformations; these factors make the redox potential difficult to calculate, so sometimes theoretical calculations are useful in this task. Further titration curves of the possible conformations,

Table 1.5 Some examples of protein used as reducing agents in metallic nanoparticle synthesis.

Nanoparticles	Protein	Reference
Iron	Peptide, oligopeptide	101
Gold	Bovine hemoglobin	102
	Pepsin	
	Glucoamylase	
	Catalase	

assuming all possibilities, normally provide good redox potential values for the possible active points.⁹⁸

The reduction process in biological media is usually carried out by a combination/cocktail of proteins. The cascade redox process consists in three main steps: in a first stage, the starting material is reduced by a specific protein to a reduced species that is afterwards reduced to a second species that is easier to reduce to another more specific protein in a better controlled manner. Finally, the colloidal nanomaterial yielded is stabilized in most of the cases by the same proteins involved in the redox process.

Metalloproteins are involved in multiple electron transfer (redox) bioprocesses and can be used as fine-tuned reducing agents for nanoparticle synthesis. The most promising are cupredoxins,⁹⁹ cytochromes, and iron-sulfur proteins. Each has their reduction potential depending on the type of their metallic center, the ligands which can modify not only the structure but also the electronic properties, and the secondary interaction out of the coordination sphere.¹⁰⁰

Peptides and oligopeptides can also be efficient reducing agents for nanoparticle synthesis, even at laboratory conditions. For example, the reduction pathway of Fe(II) ions to atomic metallic Fe nanoparticles by amino acid groups has been proposed in the literature. The mechanism proposed is based on the complexation of the ionic species by the amine groups and the consecutive oxidation of the amino acid. Finally, a formiate group and Fe(0) species were produced in a concerted mechanism.¹⁰¹

The amino acid sequence may affect the protein's ability to chelate and reduce metal ions. Besides the main chain, the lateral groups are essential to ensure an effective binding of metal ions and could influence the potential reduction of the peptide, protein, or oligopeptide. Namely, if the interactions between the ionic metals with the amino acid groups are strong, the reduction of the ion will need more energy; thus, the reduction could be inhibited. On the other hand, if the interaction ion/metal is too weak, the ion may not be retained and the reductions will not take place (Table 1.5).

References

1. S. Ahmed, Annu, S. Ikram and S. Yudha, Biosynthesis of gold nanoparticles: A green approach, *J. Photochem. Photobiol., B*, 2016, **161**, 141–153.
2. M. T. Rahman and E. V. Rebrov, Microreactors for gold nanoparticles synthesis: From faraday to flow, *Processes*, 2014, **2**, 466–493.

3. J. Singh, T. Dutta, K. H. Kim, M. Rawat, P. Samddar and P. Kumar, 'Green' synthesis of metals and their oxide nanoparticles: Applications for environmental remediation, *J. Nanobiotechnol.*, 2018, **16**, 1–24.
4. P. F. M. De Oliveira, A. A. L. Michalchuk, J. Marquardt, T. Feiler, C. Prinz, R. M. Torresi, P. H. C. Camargo and F. Emmerling, Investigating the role of reducing agents on mechanosynthesis of Au nanoparticles, *CrystEngComm*, 2020, **22**, 6261–6267.
5. Y. Li, Y. Cao and D. Jia, A general strategy for synthesis of metal nanoparticles by a solid-state redox route under ambient conditions, *J. Mater. Chem. A*, 2014, **2**, 3761–3765.
6. M. P. Pileni, The role of soft colloidal templates in controlling the size and shape of inorganic nanocrystals, *Nat. Mater.*, 2003, **2**, 145–150.
7. B. L. Cushing, V. L. Kolesnichenko and C. J. O'Connor, Recent advances in the liquid-phase syntheses of inorganic nanoparticles, *Chem. Rev.*, 2004, **104**, 3893–3946.
8. I. Capek, *Adv. Colloid Interface Sci.*, 2004, **110**, 49–74.
9. J. Eastoe, M. J. Hollamby and L. Hudson, *Adv. Colloid Interface Sci.*, 2006, **128–130**, 5–15.
10. F. Fievet, S. Ammar-Merah, R. Brayner, F. Chau, M. Giraud, F. Mammerti, J. Peron, J. Y. Piquemal, L. Sicard and G. Viau, The polyol process: a unique method for easy access to metal nanoparticles with tailored sizes, shapes and compositions, *Chem. Soc. Rev.*, 2018, **47**, 5187–5233.
11. T. D. Nguyen, *Nanoscale*, 2013, **5**, 9455–9482.
12. V. S. Chopra, D. A. Hendrix, L. J. Core, C. Tsui, J. T. Lis and M. Levine, The Polycomb Group Mutant *esc* Leads to Augmented Levels of Paused Pol II in the *Drosophila* Embryo, *Mol. Cell*, 2011, **42**, 837–844.
13. F. Fievet, J. P. Lagier, B. Blin, B. Beaudoin and M. Figlarz, Homogeneous and heterogeneous nucleations in the polyol process for the preparation of micron and submicron size metal particles, *Solid State Ionics*, 1989, **32–33**, 198–205.
14. F. Fievet, F. Fievet-Vincent, J. P. Lagler, B. Dumont and M. Figlarz, Controlled nucleation and growth of micrometre-size copper particles prepared by the polyol process, *J. Mater. Chem.*, 1993, **3**, 627–632.
15. Y. Xia, Y. Xiong, B. Lim and S. E. Skrabalak, *Angew. Chem., Int. Ed.*, 2009, **48**, 60–103.
16. V. K. Lamer and R. H. Dinegar, Theory, Production and Mechanism of Formation of Monodispersed Hydrosols, *J. Am. Chem. Soc.*, 1950, **72**, 4847–4854.
17. S. E. Skrabalak, B. J. Wiley, M. Kim, E. V. Formo and Y. Xia, On the polyol synthesis of silver nanostructures: Glycolaldehyde as a reducing agent, *Nano Lett.*, 2008, **8**, 2077–2081.
18. P. Y. Silvert and K. Tekaia-Elhsissen, Synthesis of monodisperse submicronic gold particles by the polyol process, *Solid State Ionics*, 1995, **82**, 53–60.
19. P. Y. Silvert, R. Herrera-Urbina and K. Tekaia-Elhsissen, Preparation of colloidal silver dispersions by the polyol process Part 2. - Mechanism of particle formation, *J. Mater. Chem.*, 1997, **7**, 293–299.

20. C. Ducamp-Sanguesa, R. Herrera-Urbina and M. Figlarz, Fine palladium powders of uniform particle size and shape produced in ethylene glycol, *Solid State Ionics*, 1993, **63–65**, 25–30.
21. F. Bonet, V. Delmas, S. Grugeon, R. Herrera Urbina, P. Y. Silvert and K. Tekaia-Elhsissen, Synthesis of monodisperse Au, Pt, Pd, Ru and Ir nanoparticles in ethylene glycol, *Nanostruct. Mater.*, 1999, **11**, 1277–1284.
22. F. Bonet, C. Guéry, D. Guyomard, R. Herrera Urbina, K. Tekaia-Elhsissen and J. M. Tarascon, Electrochemical reduction of noble metal species in ethylene glycol at platinum and glassy carbon rotating disk electrodes, *Solid State Ionics*, 1999, **126**, 337–348.
23. C. Li, W. Cai, B. Cao, F. Sun, Y. Li, C. Kan and L. Zhang, Mass synthesis of large, single-crystal Au nanosheets based on a polyol process, *Adv. Funct. Mater.*, 2006, **16**, 83–90.
24. C. Kan, C. Wang, H. Li, J. Qi, J. Zhu, Z. Li and D. Shi, Gold microplates with well-defined shapes, *Small*, 2010, **6**, 1768–1775.
25. D. Seo, C. Il Yoo, I. S. Chung, S. M. Park, S. Ryu and H. Song, Shape adjustment between multiply twinned and single-crystalline polyhedral gold nanocrystals: Decahedra, icosahedra, and truncated tetrahedra, *J. Phys. Chem. C*, 2008, **112**, 2469–2475.
26. D. Seo, C. P. Ji and H. Song, Polyhedral gold nanocrystals with Oh symmetry: From octahedra to cubes, *J. Am. Chem. Soc.*, 2006, **128**, 14863–14870.
27. S. J. Lee, G. Park, D. Seo, D. Ka, S. Y. Kim, I. S. Chung and H. Song, Coordination power adjustment of surface-regulating polymers for shaping gold polyhedral nanocrystals, *Chem. - Eur. J.*, 2011, **17**, 8466–8471.
28. C. Ducamp-Sanguesa, R. Herrera-Urbina and M. Figlarz, Synthesis and characterization of fine and monodisperse silver particles of uniform shape, *J. Solid State Chem.*, 1992, **100**, 272–280.
29. Y. Sun and Y. Xia, Shape-controlled synthesis of gold and silver nanoparticles, *Science*, 2002, **298**, 2176–2179.
30. Y. Sun and Y. Xia, Mechanistic Study on the Replacement Reaction between Silver Nanostructures and Chloroauric Acid in Aqueous Medium, *J. Am. Chem. Soc.*, 2004, **126**, 3892–3901.
31. Y. Sun, B. Mayers and Y. Xia, Metal nanostructures with hollow interiors, *Adv. Mater.*, 2003, **15**, 641–646.
32. Y. Sun, B. Mayers, T. Herricks and Y. Xia, Polyol synthesis of uniform silver nanowires: A plausible growth mechanism and the supporting evidence, *Nano Lett.*, 2003, **3**, 955–960.
33. B. J. Wiley, Y. Xiong, Z. Y. Li, Y. Yin and Y. Xia, Right bipyramids of silver: A new shape derived from single twinned seeds, *Nano Lett.*, 2006, **6**, 765–768.
34. B. Wiley, Y. Sun, B. Mayers and Y. Xia, *Chem. - Eur. J.*, 2005, **11**, 454–463.
35. Y. Sun, Y. Yin, B. T. Mayers, T. Herricks and Y. Xia, Uniform silver nanowires synthesis by reducing AgNO₃ with ethylene glycol in the presence of seeds and poly(vinyl pyrrolidone), *Chem. Mater.*, 2002, **14**, 4736–4745.

36. S. Bae, H. Han, J. G. Bae, E. Y. Lee, S. H. Im, D. H. Kim and T. S. Seo, Growth of Silver Nanowires from Controlled Silver Chloride Seeds and Their Application for Fluorescence Enhancement Based on Localized Surface Plasmon Resonance, *Small*, 2017, **13**, 1603392.
37. G. Viau, J. Y. Piquemal, M. Esparrica, D. Ung, N. Chakroune, F. Warmont and F. Fiévet, Formation of assembled silver nanowires by reduction of silver thiolate in polyol/toluene medium, *Chem. Commun.*, 2003, **3**, 2216–2217.
38. J. Y. Piquemal, G. Viau, P. Beaunier, F. Bozon-Verduraz and F. Fiévet, One-step construction of silver nanowires in hexagonal mesoporous silica using the polyol process, *Mater. Res. Bull.*, 2003, **38**, 389–394.
39. Z. Yin, H. Zheng, D. Ma and X. Bao, Porous Palladium nanoflowers that have enhanced methanol electro-oxidation activity, *J. Phys. Chem. C*, 2009, **113**, 1001–1005.
40. Y. Xiong, J. Chen, B. Wiley, Y. Xia, S. Aloni and Y. Yin, Understanding the role of oxidative etching in the polyol synthesis of Pd nanoparticles with uniform shape and size, *J. Am. Chem. Soc.*, 2005, **127**, 7332–7333.
41. Y. Xiong, J. M. McLellan, J. Chen, Y. Yin, Z. Y. Li and Y. Xia, Kinetically controlled synthesis of triangular and hexagonal nanoplates of palladium and their SPR/SERS properties, *J. Am. Chem. Soc.*, 2005, **127**, 17118–17127.
42. Y. Xiong, J. Chen, B. Wiley, Y. Xia, Y. Yin and Z. Y. Li, Size-dependence of surface plasmon resonance and oxidation for Pd nanocubes synthesized via a seed etching process, *Nano Lett.*, 2005, **5**, 1237–1242.
43. A. Chen and P. Holt-Hindle, Platinum-based nanostructured materials: Synthesis, properties, and applications, *Chem. Rev.*, 2010, **110**, 3767–3804.
44. C. Dablemont, P. Lang, C. Mangeney, J. Y. Piquemal, V. Petkov, F. Herbst and G. Viau, FTIR and XPS study of Pt nanoparticle functionalization and interaction with alumina, *Langmuir*, 2008, **24**, 5832–5841.
45. J. Chen, B. Lim, E. P. Lee and Y. Xia, *Nano Today*, 2009, **4**, 81–95.
46. H. Song, F. Kim, S. Connor, G. A. Somorjai and P. Yang, Pt nanocrystals: Shape control and Langmuir-Blodgett monolayer formation, *J. Phys. Chem. B*, 2005, **109**, 188–193.
47. Y. Wang, J. Ren, K. Deng, L. Gui and Y. Tang, Preparation of tractable platinum, rhodium, and ruthenium nanoclusters with small particle size in organic media, *Chem. Mater.*, 2000, **12**, 1622–1627.
48. J. Chen, T. Herricks and Y. Xia, Polyol synthesis of platinum nanostructures: Control of morphology through the manipulation of reduction kinetics, *Angew. Chem., Int. Ed.*, 2005, **44**, 2589–2592.
49. J. Chen, T. Herricks, M. Geissler and Y. Xia, Single-crystal nanowires of platinum can be synthesized by controlling the reaction rate of a polyol process, *J. Am. Chem. Soc.*, 2004, **126**, 10854–10855.
50. N. F. Yu, N. Tian, Z. Y. Zhou, L. Huang, J. Xiao, Y. H. Wen and S. G. Sun, Electrochemical synthesis of tetrahedral rhodium nanocrystals with extraordinarily high surface energy and high electrocatalytic activity, *Angew. Chem., Int. Ed.*, 2014, **53**, 5097–5101.

51. Y. Zhang, M. E. Grass, J. N. Kuhn, F. Tao, S. E. Habas, W. Huang, P. Yang and G. A. Somorjai, Highly selective synthesis of catalytically active monodisperse rhodium nanocubes, *J. Am. Chem. Soc.*, 2008, **130**, 5868–5869.
52. A. J. Biacchi and R. E. Schaak, The solvent matters: kinetic versus thermodynamic shape control in the polyol synthesis of rhodium nanoparticles, *ACS Nano*, 2011, **5**, 8089–8099.
53. A. J. Biacchi and R. E. Schaak, Ligand-induced fate of embryonic species in the shape-controlled synthesis of rhodium nanoparticles, *ACS Nano*, 2015, **9**, 1707–1720.
54. H. Zhang, M. Jin and Y. Xia, *Angew. Chem., Int. Ed.*, 2012, **51**, 7656–7673.
55. S. Xie, N. Lu, Z. Xie, J. Wang, M. J. Kim and Y. Xia, Synthesis of Pd-Rh core-frame concave nanocubes and their conversion to Rh cubic nanoframes by selective etching of the Pd cores, *Angew. Chem., Int. Ed.*, 2012, **51**, 10266–10270.
56. G. Viau, R. Brayner, L. Poul, N. Chakroune, E. Lacaze, F. Fiévet-Vincent and F. Fiévet, Ruthenium nanoparticles: Size, shape, and self-assemblies, *Chem. Mater.*, 2003, **15**, 486–494.
57. R. Harpeness, Z. Peng, X. Liu, V. G. Pol, Y. Koltypin and A. Gedanken, Controlling the agglomeration of anisotropic Ru nanoparticles by the microwave-polyol process, *J. Colloid Interface Sci.*, 2005, **287**, 678–684.
58. X. Yan, H. Liu and K. Y. Liew, Size control of polymer-stabilized ruthenium nanoparticles by polyol reduction, *J. Mater. Chem.*, 2001, **11**, 3387–3391.
59. T. Audichon, B. Guenot, S. Baranton, M. Cretin, C. Lamy and C. Coutanceau, Preparation and characterization of supported RuIr(1-x) O₂ nano-oxides using a modified polyol synthesis assisted by microwave activation for energy storage applications, *Appl. Catal., B*, 2017, **200**, 493–502.
60. F. Karimi and B. A. Peppley, Comparison of conventional versus microwave heating for polyol synthesis of supported iridium based electrocatalyst for polymer electrolyte membrane water electrolysis, *Int. J. Hydrogen Energy*, 2017, **42**, 5083–5094.
61. T. L. Doane and C. Burda, The unique role of nanoparticles in nanomedicine: Imaging, drug delivery and therapy, *Chem. Soc. Rev.*, 2012, **41**, 2885–2911.
62. T. S. Rodrigues, M. Zhao, T. H. Yang, K. D. Gilroy, A. G. M. da Silva, P. H. C. Camargo and Y. Xia, Synthesis of Colloidal Metal Nanocrystals: A Comprehensive Review on the Reductants, *Chem. - A Eur. J.*, 2018, **24**, 16944–16963.
63. L. J. Grady and J. R. Polimeni, *Discrete Calculus: Applied Analysis on Graphs for Computational Science*, 2010, pp. 1–366.
64. H. Shirakawa, E. J. Louis, A. G. MacDiarmid, C. K. Chiang and A. J. Heeger, Synthesis of electrically conducting organic polymers: Halogen derivatives of polyacetylene, (CH)_x, *J. Chem. Soc., Chem. Commun.*, 1977, 578–580.

65. C. K. Chiang, M. A. Druy, S. C. Gau, A. J. Heeger, E. J. Louis, A. G. MacDiarmid, Y. W. Park and H. Shirakawa, Synthesis of Highly Conducting Films of Derivatives of Polyacetylene, (CH)_x, *J. Am. Chem. Soc.*, 1978, **100**, 1013–1015.
66. X. Lin, B. Wegner, K. M. Lee, M. A. Fusella, F. Zhang, K. Moudgil, B. P. Rand, S. Barlow, S. R. Marder, N. Koch and A. Kahn, Beating the thermodynamic limit with photo-activation of n-doping in organic semiconductors, *Nat. Mater.*, 2017, **16**, 1209–1215.
67. E. Dalcanale, R. Pinalli and D. Chimica, *Encyclopedia of Polymeric Nanomaterials*, 2015.
68. K. Gurunathan, A. V. Murugan, R. Marimuthu, U. P. Mulik and D. P. Amalnerkar, Electrochemically synthesized conducting polymeric materials for applications towards technology in electronics, optoelectronics and energy storage devices, *Mater. Chem. Phys.*, 1999, **61**, 173–191.
69. X. Nie, T. Xiao and Z. Liu, A redox-generated biomimetic membrane potential across polypyrrole films, *Chem. Commun.*, 2019, **55**, 10023–10026.
70. R. Prakash, Electrochemistry of polyaniline: Study of the pH effect and electrochromism, *J. Appl. Polym. Sci.*, 2002, **83**, 378–385.
71. M. J. Greaney, S. Das, D. H. Webber, S. E. Bradforth and R. L. Brutchey, Improving open circuit potential in hybrid P3HT: CdSe bulk heterojunction solar cells via colloidal tert-butylthiol ligand exchange, *ACS Nano*, 2012, **6**, 4222–4230.
72. J. D. Stenger-Smith, R. W. Lenz and G. Wegner, Spectroscopic and cyclic voltammetric studies of poly(*p*-phenylene vinylene) prepared from two different sulphonium salt precursor polymers, *Polymer*, 1989, **30**, 1048–1053.
73. W. Li, Q. X. Jia and H. L. Wang, Facile synthesis of metal nanoparticles using conducting polymer colloids, *Polymer*, 2006, **47**, 23–26.
74. F. Najafi, N. Ghasemian, M. Safari and M. Salami-Kalajahi, Poly(propylene imine) dendrimer as reducing agent for chloroauric acid to fabricate and stabilize gold nanoparticles, *J. Phys. Chem. Solids*, 2021, **148**, 109682.
75. M. N. Nadagouda and R. S. Varma, Synthesis of thermally stable carboxymethyl cellulose/metal biodegradable nanocomposites for potential biological applications, *Biomacromolecules*, 2007, **8**, 2762–2767.
76. H. Duan, D. Wang and Y. Li, Green chemistry for nanoparticle synthesis, *Chem. Soc. Rev.*, 2015, **44**, 5778–5792.
77. J. N. Barboza, C. da Silva Maia Bezerra Filho, R. O. Silva, J. V. R. Medeiros and D. P. de Sousa, An overview on the anti-inflammatory potential and antioxidant profile of eugenol, *Oxid. Med. Cell. Longevity*, 2018, **2018**, 1–9.
78. V. Tekin, O. Kozgus Guldu, E. Dervis, A. Yurt Kilcar, E. Uygur and F. Z. Biber Muftuler, Green synthesis of silver nanoparticles by using eugenol and evaluation of antimicrobial potential, *Appl. Organomet. Chem.*, 2019, **33**, 1–7.

79. I. Bibi, N. Nazar, S. Ata, M. Sultan, A. Ali, A. Abbas, K. Jilani, S. Kamal, F. M. Sarim, M. I. Khan, F. Jalal and M. Iqbal, Green synthesis of iron oxide nanoparticles using pomegranate seeds extract and photocatalytic activity evaluation for the degradation of textile dye, *J. Mater. Res. Technol.*, 2019, **8**, 6115–6124.
80. M. Herlekar, S. Barve and R. Kumar, Plant-Mediated Green Synthesis of Iron Nanoparticles, *J. Nanopart.*, 2014, **2014**, 1–9.
81. T. Y. Suman, S. R. Radhika Rajasree, R. Ramkumar, C. Rajthilak and P. Perumal, The Green synthesis of gold nanoparticles using an aqueous root extract of *Morinda citrifolia* L, *Spectrochim. Acta, Part A*, 2014, **118**, 11–16.
82. J. K. Andeani, H. Kazemi, S. Mohsenzadeh and A. Safavi, Biosynthesis of gold nanoparticles using dried flowers extract of *Achillea wilhelmsii* plant, *Dig. J. Nanomater. Bios.*, 2011, **6**, 1011–1017.
83. G. Zhan, J. Huang, M. Du, I. Abdul-Rauf, Y. Ma and Q. Li, Green synthesis of Au-Pd bimetallic nanoparticles: Single-step bioreduction method with plant extract, *Mater. Lett.*, 2011, **65**, 2989–2991.
84. D. Garibo, H. A. Borbón-Nuñez, J. N. D. de León, E. García Mendoza, I. Estrada, Y. Toledano-Magaña, H. Tiznado, M. Ovalle-Marroquin, A. G. Soto-Ramos, A. Blanco, J. A. Rodríguez, O. A. Romo, L. A. Chávez-Almazán and A. Susarrey-Arce, Green synthesis of silver nanoparticles using *Lysiloma acapulcensis* exhibit high-antimicrobial activity, *Sci. Rep.*, 2020, **10**, 1–11.
85. N. Krithiga, A. Rajalakshmi and A. Jayachitra, Green Synthesis of Silver Nanoparticles Using Leaf Extracts of *Clitoria ternatea* and *Solanum nigrum* and Study of Its Antibacterial Effect against Common Nosocomial Pathogens, *J. Nanosci.*, 2015, **2015**, 1–8.
86. M. Naseer, U. Aslam, B. Khalid and B. Chen, Green route to synthesize Zinc Oxide Nanoparticles using leaf extracts of *Cassia fistula* and *Melia azadarach* and their antibacterial potential, *Sci. Rep.*, 2020, **10**, 1–10.
87. M. F. Al-Hakkani, Biogenic copper nanoparticles and their applications: A review, *SN Appl. Sci.*, 2020, **2**, 505.
88. Z. Vaseghi, A. Nematollahzadeh and O. Tavakoli, Green methods for the synthesis of metal nanoparticles using biogenic reducing agents: A review, *Rev. Chem. Eng.*, 2018, **34**, 529–559.
89. K. B. Narayanan and N. Sakthivel, Biological synthesis of metal nanoparticles by microbes, *Adv. Colloid Interface Sci.*, 2010, **156**, 1–13.
90. M. Gericke and A. Pinches, Biological synthesis of metal nanoparticles, *Hydrometallurgy*, 2006, **83**, 132–140.
91. R. Prasad, V. Kumar, M. Kumar and S. Wang, *Fungal Nanobionics: Principles and Applications*, 2018.
92. M. R. Salvadori, R. A. Ando, C. A. O. Nascimento and B. Corrêa, Dead biomass of Amazon yeast: A new insight into bioremediation and recovery of silver by intracellular synthesis of nanoparticles, *J. Environ. Sci. Health A*, 2017, **52**, 1112–1120.

93. C. Li, W. Jiang, N. Ma, Y. Zhu, X. Dong, D. Wang, X. Meng and Y. Xu, Bioaccumulation of cadmium by growing *Zygosaccharomyces rouxii* and *Saccharomyces cerevisiae*, *Bioresour. Technol.*, 2014, **155**, 116–121.
94. D. R. Majumder, Bioremediation: Copper Nanoparticles from Electronic-waste, *Int. J. Eng. Sci. Technol.*, 2012, **4**, 4380–4389.
95. M. H. Fulekar, J. Sharma and A. Tendulkar, Bioremediation of heavy metals using biostimulation in laboratory bioreactor, *Environ. Monit. Assess.*, 2012, **184**, 7299–7307.
96. E. Priyadarshini, S. S. Priyadarshini and N. Pradhan, Heavy metal resistance in algae and its application for metal nanoparticle synthesis, *Appl. Microbiol. Biotechnol.*, 2019, **103**, 3297–3316.
97. S. Prabhulkar, H. Tian, X. Wang, J. J. Zhu and C. Z. Li, Engineered proteins: Redox properties and their applications, *Antioxid. Redox Signaling*, 2012, **17**, 1796–1822.
98. G. M. Ullmann and E. Bombarda, PKa values and redox potentials of proteins. What do they mean?, *Biol. Chem.*, 2013, **394**, 611–619.
99. R. K. Bains and J. J. Warren, A single protein redox ruler, *Proc. Natl. Acad. Sci. U. S. A.*, 2016, **113**, 248–250.
100. P. Hosseinzadeh and Y. Lu, Design and fine-tuning redox potentials of metalloproteins involved in electron transfer in bioenergetics, *Biochim. Biophys. Acta, Bioenerg.*, 2016, **1857**, 557–581.
101. K. Klačanová, P. Fodran, P. Šimon, P. Rapta, R. Boča, V. Jorík, M. Migliorini, E. Kolek and L. Čaplovič, Formation of Fe(0)-Nanoparticles via Reduction of Fe(II) Compounds by Amino Acids and Their Subsequent Oxidation to Iron Oxides, *J. Chem.*, 2013, **2013**, 961629.
102. Y. Leng, L. Fu, L. Ye, B. Li, X. Xu, X. Xing, J. He, Y. Song, C. Leng, Y. Guo, X. Ji and Z. Lu, Protein-directed synthesis of highly monodispersed, spherical gold nanoparticles and their applications in multidimensional sensing, *Sci. Rep.*, 2016, **6**, 1–11.